Investigation of dimensional and geometrical tolerances of laser powder directed energy deposition process

Precision Engineering 85 (2024) 217–225

Contents lists available at ScienceDirect

Precision Engineering

journal homepage: www.elsevier.com/locate/precision

Investigation of dimensional and geometrical tolerances of laser powder directed energy deposition process

Gabriele Piscopo *, Alessandro Salmi, Eleonora Atzeni

Department of Management and Production Engineering, Politecnico di Torino, Italy

ARTICLE INFO

Handling Editor: Prof. R. Leach

Keywords:
Additive manufacturing
Directed energy deposition
Laser metal deposition
Surface quality
Dimensional tolerances
Geometrical tolerances

ABSTRACT

Laser Powder Directed Energy Deposition (LP-DED) is a promising Additive Manufacturing (AM) technology that offers the opportunity of repairing and revamping damaged or outdated parts and molds. Notwithstanding, it should be considered that the low surface quality of the produced parts makes post-processing operations necessary in order to meet the industrial requirements, and these operations strongly depend on the accuracy of the produced parts. In this paper, firstly an artifact for the LP-DED process, including classical features with and without curvatures, is proposed. Then, the dimensional accuracy and geometrical tolerances of the features are evaluated, limited to AISI 316L stainless steel.

The findings of this work showed that the dimensional and geometrical tolerances of the LP-DED process are comparable with those of sand casting. On the other hand, tolerances are lower compared to Laser Beam Powder Bed Fusion (LB-PBF) technologies but are similar to those observed in Electron Beam Powder Bed Fusion (EB-PBF).

1. Introduction

Additive Manufacturing (AM) technologies are nowadays used in several sectors, from biomedical to aerospace [1–3], from automotive to repair [4–6], from navy to robotics [7,8]. AM technologies include several processes which differ from each other for the material used (polymeric, ceramic and metallic) and for the joining mechanism which is used to bond the material to form a part [9–11]. Considering the metal AM processes the major classification concerns the material addition method [9]. In this context, it is possible to identify two process families that are the Powder Bed Fusion (PBF) and the Directed Energy Deposition (DED) [6,9,12]. PBF processes are mainly classified as Laser Beam Powder Bed Fusion (LB-PBF) and Electron Beam Powder Bed Fusion (EB-PBF), based on the energy source used to melt the metal powders [10]. DED processes are classified as Powder Directed Energy Deposition (*P*-DED) and Wire Directed Energy Deposition (W-DED), based on the feedstock material.

These metal AM families are used for different applications. The main application of PBF processes is the production of high-value components, such as turbine blades [2,13], dental and orthopedic prostheses [14,15], waveguides [16] and lightweight structures [5,11]. On the contrary, DED processes are mostly used for repair and maintenance applications [6,17], surface modification [18] and Functionally Graded Materials (FGMs) [19].

Despite AM technologies are currently used for the production of final components, the main reason that curbs the growth of industrial applications is related to the quality of the obtained parts [20]. In fact, one of the main characteristics required by industries is the quality of the produced components [21], which can mainly be defined in terms of mechanical and geometrical requirements [22]. Focusing the attention on geometrical requirements, the quality, in accordance with the ISO 286–1, ISO 2768–1, ISO 2768–2 and ISO 21920-2 standards, is defined by surface roughness, dimensional accuracy, and geometrical tolerances [23–26]. The information regarding the component quality is very useful for defining and managing the material allowance necessary during the machining operations that are needed to achieve the technical requirements of the component design [27].

From a literature review, it is possible to observe that the studies on the evaluation of the geometrical quality are mainly focused on PBF processes. In detail, the surface roughness is mostly analyzed by varying the orientation of the surface, such as using horizontal, vertical and tilted surfaces [28–32] and by varying the process parameters [31, 33–35]. The investigation of surface roughness is performed on both actual manufactured components and specific artifacts. However, from

* Corresponding author.
E-mail address: gabriele.piscopo@polito.it (G. Piscopo).

https://doi.org/10.1016/j.precisioneng.2023.10.006
Received 28 December 2022; Received in revised form 4 August 2023; Accepted 15 October 2023
Available online 20 October 2023

the review by Townsend et al. [28], emerges that 90 % of characterization works in the literature are based on an artifact. The application of an artifact during process manufacturing development has to be preferred since it allows catching the capabilities of the process for different geometries prior to optimizing it [28].

Analogously, regarding dimensional accuracy, most studies analyze different features [36] along with the different building orientations of the same features [37,38], and the effect of process parameters [38–40]. Again, the dimensional accuracy of PBF processes is evaluated on final parts [41,42] or benchmark artifacts [36,40].

Regarding DED processes, studies in the literature are mainly focused on the evaluation of the surface roughness. It is noticeable that the surface roughness, Ra, typically ranges between 25 μm and 35 μm [22] and is comparable to that obtainable in EB-PBF [12]. In fact, by comparing DED and EB-PBF, even if the waviness is longer in DED, since the laser spot and the layer thickness are 10 times higher, the superimposed roughness is similar, because it is primarily influenced by adhered powder particle size [43], that is comparable in both processes. In general, smaller is the powder size, lower is the roughness value. Analogously to powder bed processes, the dimensional accuracy is dependent on the optimization of process parameters [44]. In addition, in the surface quality of DED parts is also influenced by the powder flow, and it is a rule of thumb to deposit in the powder stream focal plane [45,46]. Overall, studies in the literature suggest that components produced by the DED process are characterized by a dimensional accuracy in the order of few millimeters [22,47,48]. However, these studies are mostly based on individual features, usually cuboid geometries, or a component produced by a specific DED technology and system, and therefore cannot be generalized to other DED geometries or DED processes, as is possible by using a reference artifact. Thus, it emerges the need to evaluate the dimensional accuracy or geometrical tolerances of the DED process using an appropriate artifact and a systematic procedure [28,49,50]. This is confirmed by Izadi et al. [44], who emphasise the need to define and use a systematic protocol in order to obtain satisfactory results.

In order to design an artifact for the DED process, it is useful to first discuss the reference geometries already adopted in the literature for metal additive manufacturing processes. A review on the artifacts used in the literature to evaluate the dimensional and geometrical capabilities of AM processes was presented by Rebaioli and Fassi [51]. Analyzing the benchmark artifacts used in the literature, it is possible to point out that most of them are focused on the evaluation of the feasibility and the accuracy of small features, that are difficult if not impossible to reproduce by DED. For example, from this perspective Kruth et al. [52] analyzed and compared on different LB-PBF systems the process limitations in producing small holes, in the range 0.5 mm–5 mm of diameter, and thin walls, with a variable thickness between 0.25 mm and 1 mm. Analogously, the study of Castillo [53] used a benchmark artifact characterized by thin walls, inclined surfaces, through holes and narrow and high pin features. An artifact including curved surfaces, thin walls, small holes and cooling tubes was proposed by Abdel Ghany and Moustafa [54]. The same approach was taken by Vandenbroucke and Kruth [55], who proposed two artifacts to evaluate respectively the accuracy and the feasibility of producing small details in LB-PBF process. Moylan et al. [56] and Moylan et al. [57] designed two benchmark artifacts to be produced using both LB-PBF and EB-PBF processes, characterized by overhang features, rectangular and circular bosses and holes with small dimensions. Once again, the artifacts were specifically designed for the characterization of the process capabilities and the definition of the minimum feature spacing.

Later, Gruber et al. [58] using an artifact performed a comparison on dimensional tolerances among different PBF processes and also the *P*-DED process, and concluded that LB-PBF process is the most accurate. Nevertheless, the authors performed the analysis using a benchmark designed for PBF processes, including thin walls, narrow cavities, and internal channels not producible by DED. Noteworthy, it should be considered that the lower accuracy of DED with respect to PBF is balanced by a higher production rate [59].

In this work, the capabilities of the DED process in terms of dimensional and geometrical tolerances are investigated using a specifically designed artifact, with the aim of bridging the gap in the existing literature. The purpose is improving the knowledge and the Technology Readiness Level (TRL) of the DED process. In particular, the attention is focused on the DED processes that use a laser as energy source and metal powder as feedstock material. It is possible to refer to these processes as Laser Powder Directed Energy Deposition (LP-DED).

1.1. Artifact design

The benchmark artifact designed for this work consists of different classical features that were selected in order to evaluate both the accuracy and the geometrical capabilities of the LP-DED process. The artifact is designed based on the assumption of using the LP-DED process for repair and mold redesign applications [6,17]. In these applications, material is deposited onto a prepared surface to restore the component or add solid features, followed by machining of the repaired volume to meet the part design requirements. The focus is therefore on the tolerances of the deposited geometries to define the minimum allowance for machining operations. The classical features have been selected to allow the evaluation of flatness, straightness, circularity, parallelism, cylindricity, angularity and profile tolerances. The range of feature dimensions is defined considering as lower bound the minimum producible feature size and as upper bound the typical volume of a repair. Specifically, it is possible to state that the minimum dimension of a massive sample ranges between 2.5 and 5 times the dimension of the laser beam. Obviously, this aspect could also be applied, with appropriate considerations, to the other metal AM processes. In fact, as for the other metal AM processes [60], there is a relation between the minimum dimension and the energy beam.

In detail, the features used in the artifact can be classified into five groups that are cubes, cylinders, pyramids, cones and hemispheres. The selection of these geometries follows what is recommended in ISO 1101–2017 standard which defines the tolerances on these geometries. A characteristic dimension (L) is defined, that all groups have in common.

- cube (CU): the characteristic dimension (L) is the length of the edge;
- cylinder (CY): the characteristic dimension (L) is the diameter of the base and the height is equal to the diameter;
- pyramid (PY): the characteristic dimension (L) is the length of the square base edge and the height is equal the base edge;
- cone (CO): the characteristic dimension (L) is the diameter of the base and the height is equal to the diameter;
- hemisphere (HS): the characteristic dimension (L) is the diameter

Fig. 1 shows the characteristic length of each group and the definition of geometrical tolerances.

Three different values of the characteristic dimension (L) are 20 mm, 15 mm, and 10 mm, that fit into different ISO ranges. Consequently, a total of 15 features are included. The above mentioned features are arranged on a square base plate, thick enough to prevent distortion during deposition. The location of the features and the minimum distance between them are set to avoid interference with the deposition head and to allow for an easier 3D scan inspection.

Fig. 2 shows the CAD representation of the designed artifact used in this work. This simple design is suitable for DED processes as all the features can be easily produced, allows the process limit to be tested when approaching smaller volumes or sharp points, allows the distortion to be assessed in relation to the size of the feature or to the gradient of the deposited volume along the height, which in DED leads to significantly different thermal histories. The artifact can also be easily scaled if larger deposition volumes are of interest.

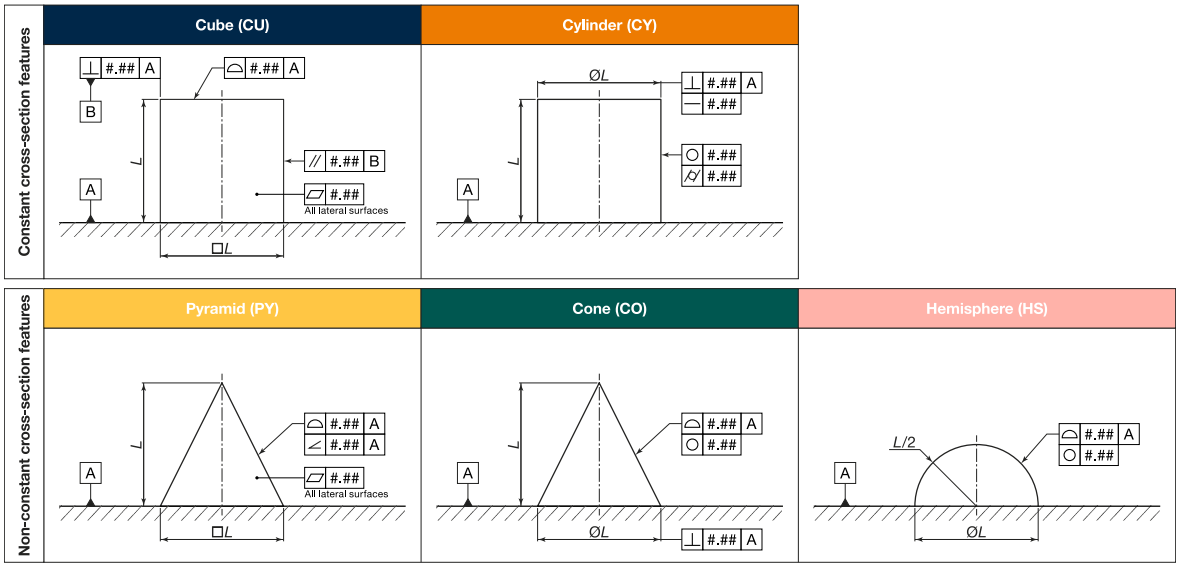

Fig. 1. Definition of characteristic length and geometrical tolerances for each group.

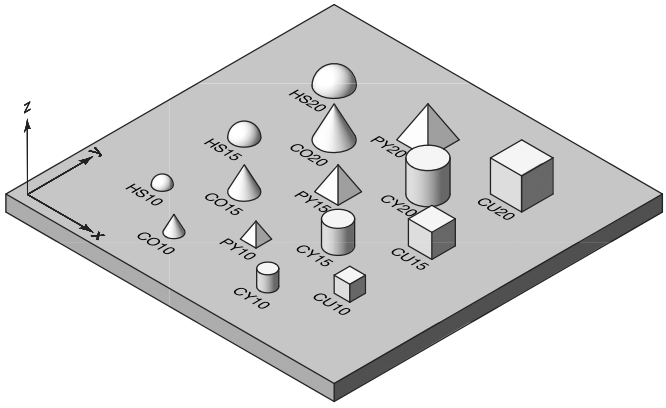

Figs. 2. 3D CAD geometry of the benchmark artifact.

1.2. Artifact production and measurement

The evaluation steps can be summarized in the artifact production, the features measurement and data analysis. In the following paragraphs, the material, the equipment, the tool and the procedure used in the experimental investigation are described.

1.3. Material and production system

The artifact was produced in AISI 316L stainless steel by using the Laserdyne 430 system by Prima Additive (Collegno, Italy). More in detail, the Laserdyne 430 system is equipped with a fiber laser with a maximum power of 1000 W and the laser beam has a top hat distribution and a diameter of 2 mm in the focal plane. The deposition head has 4 injection nozzles that generate a 4 mm powder flow spot on the same focal plane. The building volume is 585 × 408 × 508 mm^3. MetcoAdd 316L-D gas atomized powder supplied by Oerlikon Metco Inc. (Troy, MI, US) was used, with particles size ranging from 45 μm to 106 μm.

The features were deposited on a 210 × 210 × 10 mm^3 AISI 316L substrate adopting a three-axis configuration. Standard process parameters for AISI 316L stainless steel were set, which are listed in Table 1. A constant Z axis increment of 0.5 mm was programmed for the deposition process. The powder particles were delivered to the working area using a constant flux of argon of 6 L/min. Argon was also used as shielding gas for the laser beam.

Table 1
Standard process parameters of 316L stainless steel used for samples production.

Process parameter	Value	
	Contour	Filling
Laser power (W)	650	500
Travel speed (mm/min)	850	850
Powder feed rate (g/min)	11.1	11.1

The features were deposited from the biggest dimension to the smallest one, and the order used during the deposition was cube, pyramid, hemisphere, cylinder and finally cone.

1.4. Measurement and analysis

After production, samples were measured using the structured light scanner ATOS compact produced by Carl Zeiss GOM Metrology GmbH (Braunschweig, Germany). The maximum resolution of the scanner is 0.021 mm and the linear measurement error is less than 0.02 mm according to the acceptance test of VDI/VDE 2634 guideline part 3 [61]. To reduce the reflectivity of surfaces, specimens were coated with a thin layer of talc powder before scan. The application of this layer of talc powder does not influence the measurement results because the powder size is lower than scanner accuracy [62]. For each feature, the acquired point cloud, after removal of spurious data, was elaborated using the software GOM Inspect 2021 to compare the actual and the nominal geometries.

The dimensional accuracy of DED features was then evaluated in terms of IT grade according to the ISO 286-1 standard. For a given nominal dimension, the IT grade provides the manufacturing tolerances that define how precise is the manufacturing process. The IT grade is calculated based on the n value, that is the tolerance unit. In particular, for the generic k-th dimension, the corresponding tolerance unit n_k is given by equation (1):

$$n_k = \frac{1000 \bullet \left| D_{k,nom} - D_k \right|}{i} \tag{1}$$

where $D_{k,nom}$ in the k-th nominal dimension, D_k is the k-th measured dimension and i is the tolerance factor which depends on the ISO nominal dimension range, and is tabulated in Ref. [23]. The result of the elaboration is a distribution of the n_k values for each dimensional range. In order to define the maximum dimensional error of the LP-DED system

the n_k value corresponding to the 95th percentile of that distribution is used to determine the IT tolerance grade.

2. Results and discussion

After the production, the surfaces of the building platform were cleaned using isopropyl alcohol. As illustrated in Fig. 3, visual inspection showed that all the features were produced without macroscopic defects.

After cleaning operations and coating with talc powder, the artifact was fixed on a manually indexable table and was then measured using the ATOS Compact Scan 2 M. The whole geometry of the artifact was reconstructed from 100 different views from various angles. The views were registered by using reference points (markers) located on the substrate surface, thus obtaining the point cloud of the actual geometry (Fig. 4).

For each feature, the respective point cloud was extracted for further evaluation.

Firstly, the results in terms of dimensional deviations and tolerances are described and compared with the conventional manufacturing processes and with other AM processes. Then, the geometrical dimensioning and tolerancing (GD&T) rules are applied in order to quantify the geometrical error of the samples.

2.1. Dimensional deviations and tolerances

The actual and the nominal geometries of the artifact were firstly compared in order to analyze the dimensional deviations and tolerances. The point cloud and the CAD model were aligned by using the automatic pre-alignment tool in GOM Inspect, followed by a more accurate alignment by a best-fit procedure to minimize the overall error on each feature. Fig. 5 shows the colored deviation map of the actual geometry with respect to the nominal one. The substrate does not present a significant distortion, being the flatness error less than 0.2 mm. In general, the expected height of the features is obtained on constant cross-section geometries and on hemispheres regardless of the characteristic dimension, but pyramids and cones were not successfully completed. It is a matter of fact that vertexes are critical in a layerwise production and the higher layer thickness in LP-DED amplifies this issue. Consequently, the upper part of pyramids and cones was not deposited. This experimental evidence proves that geometries with dimensions lower than 2.5 times the laser spot diameter, roughly 5 mm for the used equipment, cannot be successfully produced, thus confirming the design assumptions.

A negative deviation between −0.1 mm and −0.8 mm is observed on the lateral surfaces of almost all the features. In particular, the highest deviations are obtained in non-constant cross-section features that are pyramids, cones and hemispheres.

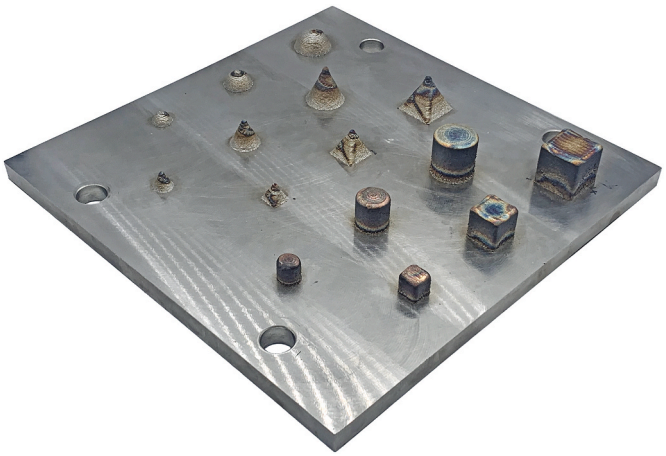

Fig. 3. LP-DED produced artifact.

As further analysis, each feature was analyzed separately. In detail, at the base of each feature, a plane normal to the building direction was created (base plane). The height of the constant cross-section features was evaluated by selecting evenly spaced points on the top surfaces and measuring the average distance from the corresponding base planes. The height of the non-constant cross-section features was evaluated by selecting the highest point of each feature and measuring its distance from the base plate. To analyze the lateral deviations, each feature was cut with m section planes parallel to the base plane; for each section k ($k = 1,2, \ldots m$) the circular or square fitting geometry was obtained and the actual diameter D_k or edge length E_k was extracted (Fig. 6). The distance between two consecutive section planes (k and $k+1$) was set to 0.2 mm in order to minimize the systematic interaction with the constant Z increment of 0.5 mm. It is worth to note that for constant cross-section features the nominal diameter or nominal edge length is the characteristic dimension of the feature itself, whereas for non-constant cross-section features the nominal diameter or nominal edge length is variable as a function of the Z level. At the end of the measurement phase, a total of 3100 values were extracted.

Fig. 7 illustrates the results of the average dimensional deviations obtained on the lateral and on the height of each feature group produced by LP-DED.

Results confirm that smaller dimensional deviations are obtained on cubes and cylinders. These features are characterized by a similar average lateral deviation of -0.49 ± 0.12 mm and an average deviation on the height of -0.11 ± 0.13 mm. The lateral deviation is independent on the characteristic length and can be easily compensated by offsetting the deposition path, thus counter-balancing the error. On the other hand, the deviation on the height falls in the typical range of metal AM processes tolerances. Pyramids and cones show the largest deviations, on average -1.12 ± 0.14 mm on the lateral and -2.00 ± 0.36 mm on the height. The average lateral deviation on hemispheres is -1.00 ± 0.13 mm and the deviation on the height is 0.21 ± 0.05 mm. The errors on the height are the consequence of the lack of deposition at vertexes. The lower lateral dimensional accuracy of pyramidal, conic and hemispheric features is attributed to the staircase effect that is an intrinsic error of AM processes on curved and inclined surfaces [63]. Moreover, a deeper analysis of the slicing algorithm of the AMXpress plugin of the MasterCam software tool revealed that the deposition path is computed considering the section in the middle of two subsequent layers [64]. The combined effect of the slicing algorithm, that underestimates the material to be added in half of the section, and the offset found on constant-section features, is the reason of the larger deviations.

All the 3100 measurements were then collected according to the nominal dimension basic sizes of ISO 2768 standard. The number of tolerance unit n_j was calculated according to equation (1), and the IT tolerance grade was evaluated considering the 95th percentile of n_j for each range of ISO basic sizes. The IT grade representative of the dimensional accuracy of the LP-DED system is thus determined for the analyzed dimension range of features. Results reveal that the overall quality (TOT) strongly depends on the basic size considered. In detail, IT16 is obtained for basic sizes up to 18 mm. For larger sizes, the tolerance grade decreases to IT14 and the process results more accurate for larger dimensions. Since the shape of the feature has a significant effect on the dimensional deviations, a further analysis is deepened by evaluating the accuracy (95th percentile of n_j) of each feature, and the obtained results are illustrated in Fig. 8.

It emerges that pyramidal and conical features exhibit the worst accuracy, with an almost constant tolerance grade of IT16 in the analyzed range.

Considering the constant cross-section feature families, that are cubes and cylinders, the IT14 tolerance grade is attributed to all the basic sizes, determining the best accuracy results. Hemispherical features show intermediate results: the IT16 is obtained for ranges up to 18 mm and IT15 for larger basic sizes.

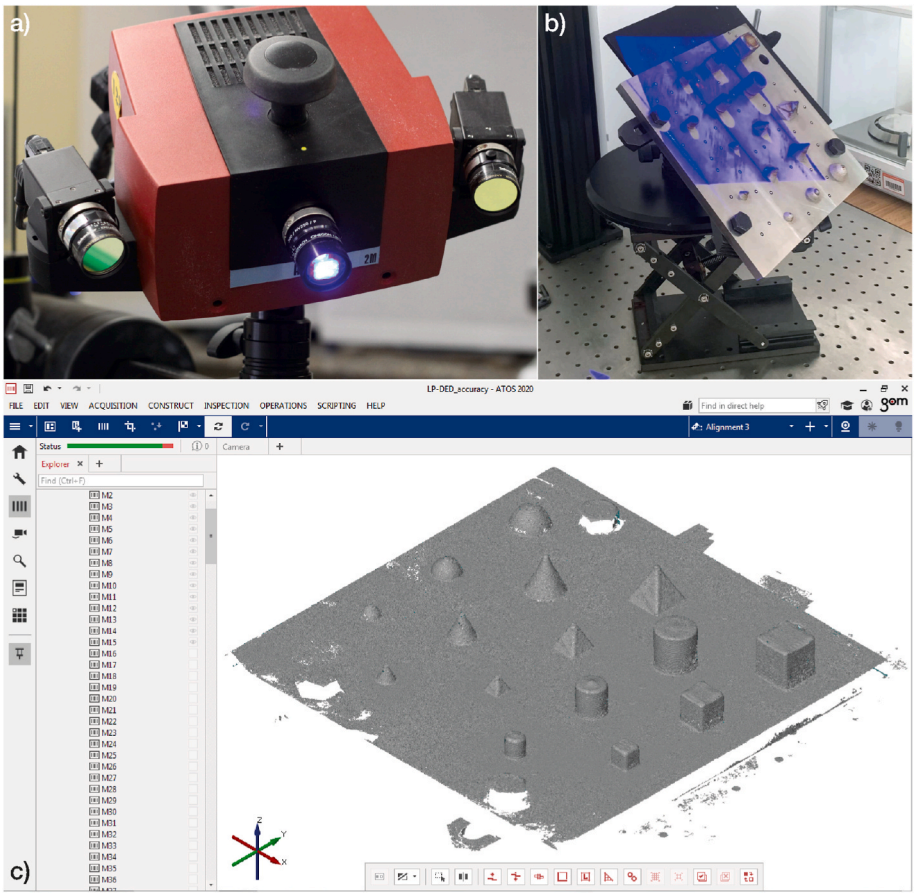

Fig. 4. Illustration of artifact point cloud acquisition: (a) ATOS Compact Scan 2 M, (b) artifact during scanning phase and (c) reconstruction of the artifact acquired views.

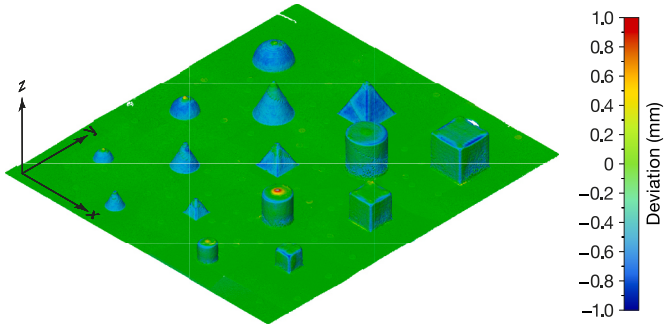

Fig. 5. Dimensional deviation map measured on LP-DED samples.

To clarify the LP-DED process positioning on metal AM processes, it is possible to state that the accuracy of the LP-DED process is lower than the one obtained in PBF processes, where either using a specific artifact [36] or test components [65,66], a maximum tolerance grade of IT13 is obtained. Table 2 compares the IT tolerance grade of the LP-DED process with IT grade values presented in the literature for other metal AM processes. It is worth noting that the dimensional accuracy of the LP-DED is closer to the one of conventional sand casting processes, in which the typical accuracy ranges from IT16 to IT18 [67].

2.2. Geometrical tolerances

Based on the features produced in this work, the form, the orientation, and the location tolerances were evaluated as in Table 3.

Fig. 9 illustrates the geometrical tolerances measured on the cubes. As expected, better results are obtained if smaller areas are considered. In detail, considering flatness, LP-DED parts show a 0.56 mm wide large tolerance zone, which covers the entire surface of each cube face, and a small tolerance zone (9×9 mm^2) that is 0.34 mm wide. Analogously, the parallelism ranges from 0.45 mm to 0.69 mm, and the perpendicularity from 0.34 mm to 0.47 mm, with better results if lateral surfaces and smaller features are considered. The surface profile measured on top surfaces is of about 0.45 mm and it is almost independent from the characteristic length.

It is worth noting that the control of the CNC machine axes ensures a high accuracy on deposition trajectory, and consequently the shape deviation is mainly caused by the irregularities in the deposited tracks, such as partially sintered particles, variations in the track width related to acceleration/deceleration of axes or changes in the powder metal flow, or presence of local agglomerates on the surface. Thus, errors on lateral surfaces are typically lower. In addition, it is observed that the cross-sections of the cube slightly diverge as the height increases, and this effect may contribute to the larger tolerance found at higher characteristic length. On the contrary, the tolerances on the top surfaces are larger since these surfaces are affected by the thermal history and deviations occurred in previous layers, and the z-increment is preprogrammed and not real-time adapted to the actual height reached on previous deposited layers. This is limited to the DED system used in the experimental campaign and, more in general, to DED systems in which an adaptive control for height compensation is not present.

The tolerances evaluated on cylinders are illustrated in Fig. 10. Again, it is clear that the characteristic length affects the straightness tolerance, and the trend is comparable to the flatness measured on cubes. It is reasonable, since the straightness relies on the axis deviation from the ideal axis line and, being the axis evaluated from the external

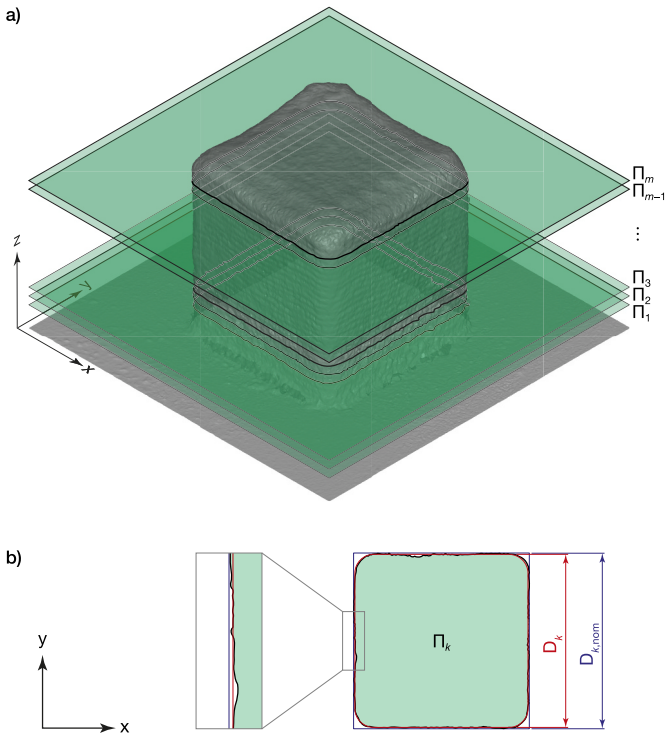

Fig. 6. Definition of the (a) section planes and (b) fitting geometry for the evaluation of dimensional deviations on lateral surfaces: nominal geometry (blue), real geometry (black) and fitting geometry (red). (For interpretation of the references to color in this figure legend, the reader is referred to the Web version of this article.)

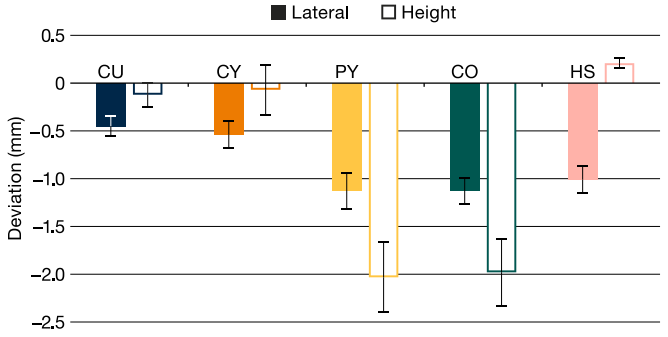

Fig. 7. Dimensional deviations of LP-DED features.

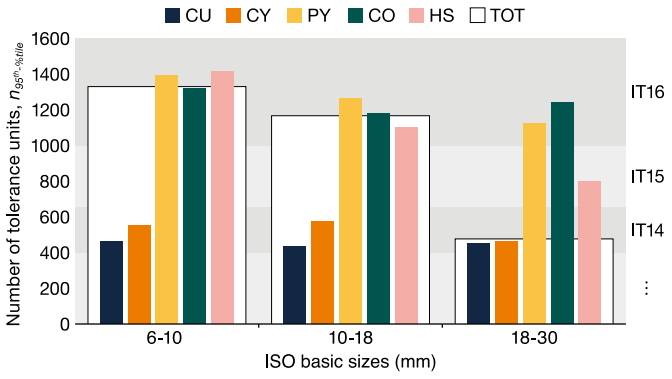

Fig. 8. Dimensional accuracy (95-th percentile) of the LP-DED samples for different ISO dimensional range.

Table 2
Comparison of IT tolerance grade of sand casting and metal AM processes.

ISO basic sizes (mm)	IT grade			
	LB-PBF	EB-PBF	Sand casting	LP-DED
6–10	IT 11 [36] IT 13 [65]	IT 13 [36]	IT16-IT18 [67]	IT 16
10–18	IT 12 [36,65]	IT 13 [36]	IT16-IT18 [67]	IT 16
18–30	IT 11 [66] IT 12 [36]	IT 13 [36]	IT16-IT18 [67]	IT 14

surface, it suffers from the same errors that characterize the external surface of the feature. In general, geometrical tolerances range from 0.1 mm to 0.43 mm, with the exception of the perpendicularity of the cylinders axes with respect to the base plane, where an error less than 0.11 mm is observed. On all the cylindrical features a circularity error of about 0.30 mm is measured. Finally, the cylindricity error is of about 0.37 mm. Again, this value is similar to flatness measured on cubes and this is justified by the fact that both, flatness and cylindricity, are related to the deposition path accuracy.

Finally, the geometrical errors measured on the other geometries are shown in Fig. 11, specifically pyramids, cones, and hemispheres. All in all, it is confirmed that geometrical errors increase with the characteristic dimension of the feature. The flatness of pyramids and the circularity of cones and hemispheres, which describe the lateral surfaces of the features, similarly range between 0.38 mm and 0.52 mm. Analogously, the angularity error measured on pyramids, which is related to the inclination of the lateral surfaces, ranges between 0.42 mm and 0.58 mm. These values are comparable with the tolerances obtained on the lateral surfaces of cubes and cylinders. The perpendicularity of the axis of the cone is also congruent to the values obtained for constant cross-section features. Additionally, pyramids, cones and hemispheres show a similar geometrical surface profile error with values that range between 0.79 mm and 1.08 mm, attributed to the stair stepping generated by the non-adaptive slicing, that emphasizes the geometric errors when the surface normal tends to be parallel to the building direction.

The findings are consistent with the typical tolerances of the EB-PBF process [36,58,68], however LP-DED tolerances are almost twice with respect to the LB-PBF tolerances [36,58,69]. However, it should be observed that the PBF measurements are based on artifacts, which, as previously introduced, are usually designed with fine details or small features, thus caution should be exercized in generalizing the findings. Table 4 compares the geometrical tolerances of LB-PBF and EB-PBF available in the literature, with the geometrical tolerances of the LP-DED process obtained in this work. Reasonably, the geometrical tolerances measured on LP-DED are comparable to tolerances in permanent mold casting, gravity and low pressure die casting which are some of the most accurate casting processes [70]. More specifically, in terms of surface profile errors, the values obtained in this work fall within grade 7 of general surface profile tolerances for casting components, which corresponds to investment casting or metallic permanent mold processes [71].

3. Conclusion

Additive Manufacturing technologies allow complex geometries to be produced, saving time and cost compared to conventional manufacturing systems. The laser Powder Directed Energy Deposition process is rapidly growing thanks to its powerful capability in terms of repair, remanufacturing and surface modification applications. However, the quality of the components is still a problem and a definition of the geometrical and dimensional performances of the process is needed. This work aims to quantify the dimensional capabilities of the LP-DED process and investigate different how different geometries affect dimensional and geometrical errors. To this purpose, a 316L stainless steel artifact is designed by varying the characteristic length of classical

Table 3
Identification of geometrical tolerances evaluated on each feature.

		Cube	Cylinder	Pyramid	Cone	Hemisphere
Form	Flatness	x		x		
	Straightness		x			
	Cylindricity		x			
	Circularity		x		x	x
Orientation	Parallelism	x				
	Perpendicularity	x	x		x	
	Angularity			x		
Location	Surface profile	x		x	x	x

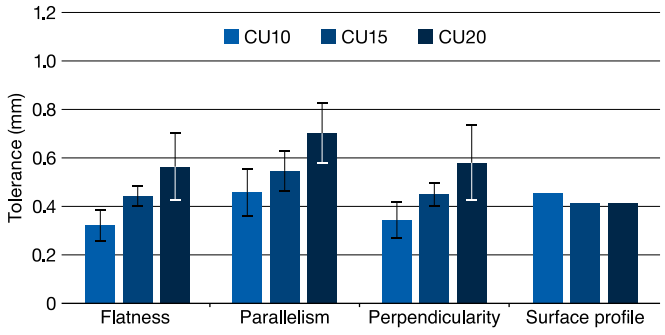

Fig. 9. Geometrical tolerances measured on cubes.

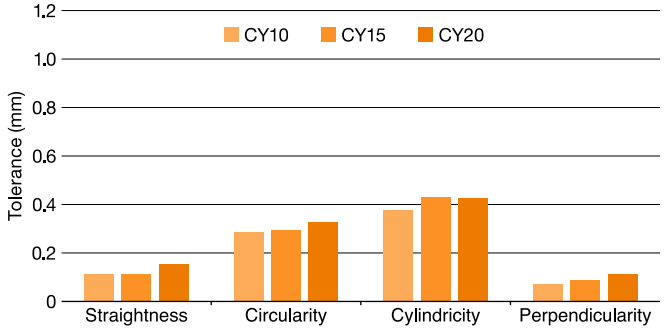

Fig. 10. Geometrical tolerances measured on cylinders.

geometries resembling DED features.

Findings limited to the analyzed characteristic length range reveal that.

- the IT tolerance grade of the LP-DED process varies between IT15 and IT17, and lower IT value is obtained for larger basic size;
- the IT tolerance grade strongly depends on the geometry of the feature. For constant cross-section geometries, an IT15 is obtained. For non-constant cross-section, where the stairstepping is distinct, the tolerance grade ranges between IT16 and IT17 with lower IT value for larger dimensions of the feature; larger features are less affected by the vertex effect, that is geometries smaller than 2.5 times the laser spot diameter cannot be successfully produced;
- considering geometrical tolerances, surface profile error is about 1 mm, angularity error is about 0.3 deg, and other geometrical tolerances are lower than 0.6 mm; higher errors are associated with larger geometries.

Summarizing the results, it is possible to conclude that for small basic size the LP-DED process is much less accurate than the PBF processes, however this gap significantly decreases when larger basic sizes are considered.

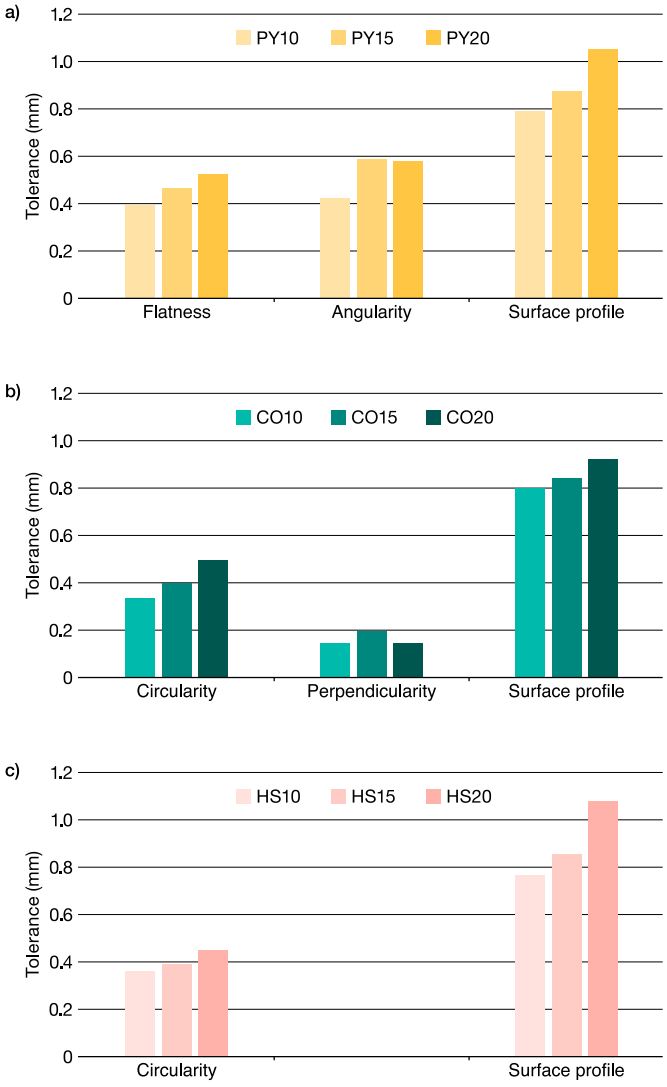

Fig. 11. Geometrical errors measured on: (a) pyramid, (b) cone and (c) hemisphere.

The procedure used in this work could be easily generalized to others directed energy deposition processes, such as Laser Wire - Directed Energy deposition (LW-DED) or Plasma Wire – Directed Energy Deposition (PW-DED). In fact, the relatively simple shapes are suitable for all the DED processes. Obviously, the minimum value of the characteristic dimension of each feature has to be related to the specific process. Based on the results obtained in this work, a suitable starting value is approximately 2.5 times the dimension of the energy source spot size or wire diameter, depending on the process used. In addition, the size, the spacing and the position of each feature could be adjusted taking into

Table 4
Comparison of geometrical tolerances of permanent mold casting and metal AM processes.

	LB-PBF	EB-PBF	Permanent mold casting	LP-DED
Flatness	0.10 [58] 0.12 [69]	0.30–0.50 [58]	0.40–0.60 [71]	0.34
Straightness		0.10 [68]	0.27–0.40 [71]	0.15
Cylindricity	0.15 [58]	0.32 [58]		0.37
Circularity	0.14 [69]			0.30
Parallelism	0.22 [69]	0.19 [68]	0.60–0.90 [71]	0.45–0.69
Perpendicularity	0.15 [58] 0.17 [69]	0.10–0.50 [58]	0.60–0.90 [71]	0.11–0.34
Angularity	0.08 [69]			0.40–0.60
Surface profile	0.09 [36]	0.13 [36]	0.76–0.86 [71]	0.45–1.08

account two main aspects, which are (i) the accessibility of the deposition head to the working area avoiding collision, and (ii) the spacing required by the measurement system used during the analysis. For example, when structured light systems are used, it is necessary to verify that the projection of the shadow of a feature does not affect the illumination of the nearby feature.

Declaration of competing interest

The authors declare that they have no known competing financial interests or personal relationships that could have appeared to influence the work reported in this paper.

References

[1] Stavropoulos P, Foteinopoulos P, Papacharalampopoulos A, Bikas H. Addressing the challenges for the industrial application of additive manufacturing: towards a hybrid solution. Int. J. Lightweight Mater. Manuf. 2018;1:157–68. https://doi.org/10.1016/j.ijlmm.2018.07.002.

[2] Liu R, Wang Z, Sparks T, Liou F, Newkirk J. Aerospace applications of laser additive manufacturing. Laser Additive Manufacturing. Woodhead Publishing; 2017. p. 351–71.

[3] Singh S, Ramakrishna S. Biomedical applications of additive manufacturing: present and future. Curr. Opin. Biomed. Eng. 2017;2:105–15. https://doi.org/10.1016/j.cobme.2017.05.006.

[4] Leal R, Barreiros FM, Alves L, Romeiro F, Vasco JC, Santos M, et al. Additive manufacturing tooling for the automotive industry. Int J Adv Manuf Technol 2017;92:1671–6. https://doi.org/10.1007/s00170-017-0239-8.

[5] Vasco JC. Additive manufacturing for the automotive industry. In: Pou J, Riveiro A, Davim JP, editors. Addit manuf. Amsterdam: Elsevier; 2021. p. 505–30.

[6] Piscopo G, Iuliano L. Current research and industrial application of laser powder directed energy deposition. Int J Adv Manuf Technol 2022;119:6893–917. https://doi.org/10.1007/s00170-021-08596-w.

[7] Frazier WE. Metal additive manufacturing: a review. J Mater Eng Perform 2014;23:1917–28. https://doi.org/10.1007/s11665-014-0958-z.

[8] Busachi A, Erkoyuncu J, Colegrove P, Drake R, Watts C, Martina F. Defining next-generation additive manufacturing applications for the ministry of defence (MoD). Proc. Cirp. 2016;55:302–7. https://doi.org/10.1016/j.procir.2016.08.029.

[9] ASTM International. ISO/ASTM 52900:2021(E) - standard terminology for additive manufacturing – general principles – terminology. ISO/ASTM 52900:2021(E). West Conshohocken (USA): ASTM International; 2021.

[10] Calignano F, Manfredi D, Ambmbrosio EP, Biamino S, Lombmbardi M, Atzeni E, et al. Overview on additive manufacturing technologies. Proc IEEE 2017;105:593–612. https://doi.org/10.1109/Jproc.2016.2625098.

[11] Gibson I, Rosen D, Stucker B. Additive manufacturing technologies. second ed. New York: Springer; 2015.

[12] Galati M. Electron beam melting process: a general overview. In: Pou J, Riveiro A, Davim JP, editors. Addit manuf. Amsterdam: Elsevier; 2021. p. 277–301.

[13] Lesyk D, Martinez S, Dzhemelinkyi V, Lamikiz A. Additive manufacturing of the superalloy turbine blades by selective laser melting: surface quality, microstructure and porosity. In: Karabegović I, editor. New technologies, development and application III. Springer Cham; 2020. p. 267–75.

[14] Dzhendov D, Dikova T. Application of selective laser melting in manufacturing of fixed dental prostheses. J. Imab. 2016;22:1414–7. https://doi.org/10.5272/jimab.2016224.1414.

[15] Rezvani Ghomi E, Khosravi F, Neisiany RE, Singh S, Ramakrishna S. Future of additive manufacturing in healthcare, vol. 17; 2021. https://doi.org/10.1016/j.cobme.2020.100255.

[16] Shen JY, Ricketts DS. Additive manufacturing of complex millimeter-wave waveguides structures using digital light processing. Ieee T Microw. Theory 2019;67:883–95. https://doi.org/10.1109/Tmtt.2018.2889452.

[17] Saboori A, Aversa A, Marchese G, Biamino S, Lombardi M, Fino P. Application of directed energy deposition-based additive manufacturing in repair. Appl. Sci.-Basel 2019;9:3316. https://doi.org/10.3390/app9163316.

[18] Kim CK, Choi SG, Kim JH, Jo HJ, Jo YC, Choi SP, et al. Characterization of surface modification by laser cladding using low melting point metal. J Ind Eng Chem 2020;87:54–9. https://doi.org/10.1016/j.jiec.2020.03.010.

[19] Ansari M, Jabari E, Toyserkani E. Opportunities and chall. Additive Manuf. Functionally Graded Metallic Mater. via Powder-fed Laser Directed Energy Deposition: Review 2021;294. https://doi.org/10.1016/j.jmatprotec.2021.117117.

[20] Majeed A, Ahmed A, Lv JX, Peng T, Muzamil M. A state-of-the-art review on energy consumption and quality characteristics in metal additive manufacturing processes. J Braz Soc Mech Sci 2020;42. https://doi.org/10.1007/s40430-020-02323-4.

[21] Dilberoglu UM, Gharehpapagh B, Yaman U, Dolen M. The role of additive manufacturing in the era of Industry 4.0. Procedia Manuf 2017;11:545–54. https://doi.org/10.1016/j.promfg.2017.07.148.

[22] Piscopo G, Salmi A, Atzeni E. Influence of high-productivity process parameters on the surface quality and residual stress state of AISI 316L components produced by directed energy deposition, vol. 30; 2021. p. 6691–702. https://doi.org/10.1007/s11665-021-05954-3.

[23] ISO 286-1. Geometrical product specifications (GPS). ISO code system for tolerances on linear sizes. Basis of tolerances, deviations and fits. BSI; 2010.

[24] ISO 2768-1. General tolerances. Tolerances for linear and angular dimensions without individual tolerance indications. BSI; 1993.

[25] ISO 2768-2. General tolerances. Geometrical tolerances for features without individual tolerance indications. 1993.

[26] ISO 21920-2. Geometrical product specifications (GPS) — surface texture: profile — Part 2: terms, definitions and surface texture parameters. BSI; 2021.

[27] Walter MS. Dimensional and geometrical tolerances in mechanical engineering–a historical review. Mach Des 2019;11:67–74.

[28] Townsend A, Senin N, Blunt L, Leach RK, Taylor JS. Surface texture metrology for metal additive manufacturing: a review. Precis Eng 2016;46:34–47. https://doi.org/10.1016/j.precisioneng.2016.06.001.

[29] Galati M, Minetola P, Rizza G. Surface roughness characterisation and analysis of the electron beam melting (EBM) process. Materials 2019;12. https://doi.org/10.3390/ma12132211.

[30] Yan XC, Gao SH, Chang C, Huang J, Khanlari K, Dong DD, et al. Effect of building directions on the surface roughness, microstructure, and tribological properties of selective laser melted Inconel 625. J Mater Process Technol 2021:288. https://doi.org/10.1016/j.jmatprotec.2020.116878.

[31] Strano G, Hao L, Everson RM, Evans KE. Surface roughness analysis, modelling and prediction in selective laser melting. J Mater Process Technol 2013;213:589–97. https://doi.org/10.1016/j.jmatprotec.2012.11.011.

[32] Newton L, Senin N, Chatzivagiannis E, Smith B, Leach R. Feature-based characterisation of Ti6Al4V electron beam powder bed fusion surfaces fabricated at different surface orientations. Addit Manuf 2020;35. https://doi.org/10.1016/j.addma.2020.101273.

[33] Koutiri I, Pessard E, Peyre P, Amlou O, De Terris T. Influence of SLM process parameters on the surface finish, porosity rate and fatigue behavior of as-built Inconel 625 parts. J Mater Process Technol 2018;255:536–46. https://doi.org/10.1016/j.jmatprotec.2017.12.043.

[34] Wang P, Sin WJ, Nai MLS, Wei J. Effects of processing parameters on surface roughness of additive manufactured Ti-6Al-4V via Electron beam melting, vol. 10; 2017. https://doi.org/10.3390/ma10101121.

[35] Safdar A, He HZ, Wei LY, Snis A, de Paz LEC. Effect of process parameters settings and thickness on surface roughness of EBM produced Ti-6Al-4V. Rapid Prototyp J 2012;18:401–8. https://doi.org/10.1108/13552541211250391.

[36] Minetola P, Galati M, Calignano F, Iuliano L, Rizza G, Fontana L. Comparison of dimensional tolerance grades for metal AM processes. Proc. CIRP 2020;88:399–404. https://doi.org/10.1016/j.procir.2020.05.069.

[37] Borrelli R, Franchitti S, Pirozzi C, Carrino L, Nele L, Polini W, et al. Ti6Al4V parts produced by electron beam melting: analysis of dimensional accuracy and surface roughness. J Adv Manuf Syst 2020;19:107–30. https://doi.org/10.1142/S0219686720500067.

[38] Kniepkamp M, Fischer J, Abele E. Dimensional accuracy of small parts manufactured by micro selective laser melting. In: 2016 international solid freeform fabrication symposium. University of Texas at Austin; 2016.

[39] Calignano F, Lorusso M, Pakkanen J, Trevisan F, Ambrosio EP, Manfredi D, et al. Investigation of accuracy and dimensional limits of part produced in aluminum alloy by selective laser melting. Int J Adv Manuf Technol 2016;88:451–8. https://doi.org/10.1007/s00170-016-8788-9.

[40] Franchitti S, Borrelli R, Pirozzi C, Carrino L, Polini W, Sorrentino L, et al. Investigation on electron beam melting: dimensional accuracy and process repeatability. Vacuum 2018;157:340–8. https://doi.org/10.1016/j.vacuum.2018.09.007.

[41] Chen J, Zhang Z, Chen X, Zhang C, Zhang G, Xu Z. Design and manufacture of customized dental implants by using reverse engineering and selective laser melting technology. J Prosthet Dent 2014;112:1088–10895. https://doi.org/10.1016/j.prosdent.2014.04.026. e1.
[42] Juechter V, Franke MM, Merenda T, Stich A, Korner C, Singer RF. Additive manufacturing of Ti-45Al-4Nb-C by selective electron beam melting for automotive applications. Addit Manuf 2018;22:118–26. https://doi.org/10.1016/j.addma.2018.05.008.
[43] Smugeresky J, Keicher D, Romero J, Griffith M, Harwell L. Laser engineered net shaping (LENS) process: optimization of surface finish and microstructural properties. Albuquerque, NM (United States): Sandia National Lab.(SNL-NM); 1997.
[44] Izadi M, Farzaneh A, Mohammed M, Gibson I, Rolfe B. A review of laser engineered net shaping (LENS) build and process parameters of metallic parts. Rapid Prototyp J 2020;26:1059–78. https://doi.org/10.1108/Rpj-04-2018-0088.
[45] Haley JC, Zheng BL, Bertoli US, Dupuy AD, Schoenung JM, Lavernia EJ. Working distance passive stability in laser directed energy deposition additive manufacturing. Mater Des 2019;161:86–94. https://doi.org/10.1016/j.matdes.2018.11.021.
[46] Zhu GX, Li DC, Zhang AF, Pi G, Tang YP. The influence of laser and powder defocusing characteristics on the surface quality in laser direct metal deposition. Opt Laser Technol 2012;44:349–56. https://doi.org/10.1016/j.optlastec.2011.07.013.
[47] Balla VK, Bose S, Bandyopadhyay A. Processing of bulk alumina ceramics using laser engineered net shaping. Int J Appl Ceram Technol 2008;5:234–42. https://doi.org/10.1111/j.1744-7402.2008.02202.x.
[48] Ma MM, Wang ZM, Wang DZ, Zeng XY. Control of shape and performance for direct laser fabrication of precision large-scale metal parts with 316L Stainless Steel. Opt Laser Technol 2013;45:209–16. https://doi.org/10.1016/j.optlastec.2012.07.002.
[49] Maleki E, Bagherifard S, Bandini M, Guagliano M. Surface post-treatments for metal additive manufacturing: progress, challenges, and opportunities. Addit Manuf 2021;37. https://doi.org/10.1016/j.addma.2020.101619.
[50] Kladovasilakis N, Charalampous P, Kostavelis I, Tzetzis D, Tzovaras D. Impact of metal additive manufacturing parameters on the powder bed fusion and direct energy deposition processes: a comprehensive review. Prog. Addit. Manuf. 2021;6:349–65. https://doi.org/10.1007/s40964-021-00180-8.
[51] Rebaioli L, Fassi I. A review on benchmark artifacts for evaluating the geometrical performance of additive manufacturing processes. Int J Adv Manuf Technol 2017;93:2571–98. https://doi.org/10.1007/s00170-017-0570-0.
[52] Kruth J-P, Vandenbroucke B, Van Vaerenbergh J, Mercelis P. Benchmarking of different SLS/SLM processes as rapid manufacturing techniques, vol. 1. 3D; 2005.
[53] Castillo L. Study about the rapid manufacturing of complex parts of stainless steel and titanium. 2005. p. 1–31.
[54] Abdel Ghany K, Moustafa SF. Comparison between the products of four. RPM Syst. Metals 2006;12:86–94. https://doi.org/10.1108/13552540610652429.
[55] Vandenbroucke B, Kruth JP. Selective laser melting of biocompatible metals for rapid manufacturing of medical parts, vol. 13; 2007. p. 196–203. https://doi.org/10.1108/13552540710776142.
[56] Moylan S, Slotwinski J, Cooke A, Jurrens K, Donmez MA. Proposal for a standardized test artifact for additive manufacturing machines and processes. In: 2012 international solid freeform fabrication symposium. University of Texas at Austin; 2012.
[57] Moylan S, Slotwinski J, Cooke A, Jurrens K, Donmez MA. An additive manufacturing test artifact, vol. 119; 2014. https://doi.org/10.6028/jres.119.017.
[58] Gruber S, Grunert C, Riede M, Lopez E, Marquardt A, Brueckner F, et al. Comparison of dimensional accuracy and tolerances of powder bed based and nozzle based additive manufacturing processes. J Laser Appl 2020;32. https://doi.org/10.2351/7.0000115.
[59] Dutta B, Froes FH. The additive manufacturing. AM) of titanium alloys 2017;72:96–106. https://doi.org/10.1016/j.mprp.2016.12.062.
[60] Emmelmann C, Herzog D, Kranz J. Design for laser additive manufacturing. Laser Additive Manufacturing; 2017. p. 259–79.
[61] Stiuso V, Minetola P, Calignano F, Galati M, Khandpur MS, Fontana L. Experimental assessment of compensated distortion in selective laser melting of Ti6Al4V parts. IOP Conf Ser Mater Sci Eng 2021:1136. https://doi.org/10.1088/1757-899x/1136/1/012048.
[62] Piscopo G, Salmi A, Atzeni E. On the quality of unsupported overhangs produced by laser powder bed fusion. Int J Manuf Res 2019;14:198–216. https://doi.org/10.1504/ijmr.2019.100012.
[63] Pérez M, García-Collado A, Carou D, Medina-Sánchez G, Dorado-Vicente R. On surface quality of engineered parts manufactured by additive manufacturing and postfinishing by machining. In: Pou J, Riveiro A, Davim JP, editors. Addit manuf. Amsterdam: Elsevier; 2021. p. 369–94.
[64] Mohan Pandey P, Venkata Reddy N, Dhande SG. Slicing procedures in layered manufacturing: a review. Rapid Prototyp J 2003;9:274–88. https://doi.org/10.1108/13552540310502185.
[65] Schmitt M, Schlick G, Schilp J. Repeatability of dimensional accuracy and mechanical properties in powder bed fusion of 16MnCr5 using a. Laser Beam 2022;114:94–9. https://doi.org/10.1016/j.procir.2022.10.013.
[66] Zongo F, Tahan A, Aidibe A, Brailovski V. Intra- and inter-repeatability of profile deviations of an AlSi10Mg tooling component manufactured by laser powder bed fusion, vol. 2; 2018. https://doi.org/10.3390/jmmp2030056.
[67] Bassoli E, Gatto A, Iuliano L, Violante MG. 3D printing technique applied to rapid casting. Rapid Prototyp J 2007;13:148–55. https://doi.org/10.1108/13552540710750898.
[68] Yang L, Anam MA. An investigation of standard test part design for additive manufacturing. In: 2014 international solid freeform fabrication symposium. University of Texas at Austin; 2014.
[69] Rupal BS, Singh T, Wolfe T, Secanell M, Qureshi AJ. Tri-planar geometric dimensioning and tolerancing characteristics of SS 316L laser powder bed fusion process test artifacts and effect of base plate removal, vol. 14; 2021. https://doi.org/10.3390/ma14133575.
[70] Swift KG, Booker JD. Casting processes. Manufacturing process selection handbook. 2013. p. 61–91.
[71] ISO 8062-3. Geometrical product specifications (GPS) — dimensional and geometrical tolerances for moulded parts. BSI; 2023.